Formation Mechanism of Micrometric Helices in Agate and Chalcedony: A Computational Analysis of Three Candidate Processes

AI4Sciences Research

ABSTRACT

Micrometric three-dimensional silica helices observed in agate and chalcedony present an open problem regarding their abiotic formation mechanism. We computationally evaluate three candidate processes: diffusion-limited aggregation (DLA), reaction-diffusion with Turing instability, and fibrous growth with lattice-mismatch twist. DLA produces fractal structures (dimension 1.455) with helicity 0.026, failing to generate true helices. Reaction-diffusion yields planar spirals (dominant wavelength 28.0) but not 3D helices. Fibrous growth produces helical structures in 8.0% of simulations with racemic chirality (right: 25%, $p = 0.289$). Morphometric discriminant analysis separating agate helices, biomorphs, and biogenic spirals achieves 83.0% accuracy, with Si/Fe ratio (weight -0.606) and regularity (0.693) as the strongest discriminators. Reaction-diffusion scores highest overall (0.400), followed by fibrous growth (0.389) and DLA (0.280), though no single mechanism fully reproduces all observed characteristics.

1 INTRODUCTION

Spiral and helical morphologies are common biosignatures in the geological record, observed in ammonites, gastropods, and microbial stalks. However, similar micrometric helices have been reported in agate and chalcedony that appear to be abiotic in origin [1]. Their composition—silica with traces of iron—and their morphological resemblance to silica-carbonate biomorph nanorod assemblies [2] raise the fundamental question of what physicochemical pathway generates these structures.

This problem has implications for astrobiology and paleontology, as the inability to distinguish abiotic helices from biogenic spirals complicates the interpretation of putative microfossils [3, 4].

We evaluate three candidate mechanisms: (1) diffusion-limited aggregation (DLA) [6] with anisotropic attachment, where silica nanoparticles aggregate under diffusion with preferential attachment along crystallographic axes; (2) reaction-diffusion with Turing-type instability [5], where coupled silica polymerization and iron-catalyzed reactions produce periodic structures; and (3) fibrous growth with twist, where oriented silica fiber growth with lattice-mismatch-induced twist generates helical morphologies.

2 METHODS

2.1 Diffusion-Limited Aggregation

We simulate DLA with 500 particles on a 3D lattice with anisotropic sticking probabilities reflecting crystallographic preferences. Fractal dimension is computed via box-counting, and helicity is quantified from the signed torsion of the aggregate backbone.

2.2 Reaction-Diffusion Model

A two-component reaction-diffusion system couples silica concentration u and iron catalyst v with Turing-type kinetics on a 2D grid. Pattern metrics include dominant wavelength via FFT, amplitude, and curl for spiral detection.

2.3 Fibrous Growth with Twist

Silica fiber growth is modeled with twist rate controlled by lattice mismatch. A parameter sweep covers 12 twist rates (0.1–5.0) and 10 noise levels (0.01–0.3), generating 120 configurations. Helix quality, pitch, and radius are measured. Chirality statistics use 100 independent fibers.

2.4 Morphometric Discrimination

We generate synthetic datasets of agate helices ($n = 100$), silica-carbonate biomorphs ($n = 100$), and biogenic spirals ($n = 100$) with characteristic distributions of pitch, radius, Si/Fe ratio, and regularity. Fisher LDA provides discriminant projection and classification accuracy.

3 RESULTS

3.1 DLA

DLA produces fractal aggregates with fractal dimension 1.455 and helicity 0.026, confirming that diffusion-limited growth generates branching rather than helical structures. The mean radius is 3.973 with aspect ratio 3.084.

3.2 Reaction-Diffusion

The reaction-diffusion model generates planar spiral patterns (has_spiral = true) with dominant wavelength evolving from 13.067 to 28.0 over 2000 steps. However, these are 2D patterns, not 3D helices (is_3d_helix = false).

3.3 Fibrous Growth

Fibrous growth produces helical structures in 8 of 100 fibers (8.0%). Among helical fibers, chirality is racemic: 6 left-handed, 2 right-handed (right fraction 0.25, binomial $p = 0.289$), consistent with an abiotic mechanism lacking chiral bias. Mean helix quality is 0.155 with mean pitch 0.026 and mean radius 0.010.

3.4 Mechanism Comparison

Reaction-diffusion ranks first (0.400), followed closely by fibrous growth (0.389) and DLA (0.280). No mechanism achieves high scores across all criteria.

Table 1: Mechanism comparison scores across five criteria (0–1 scale).

Criterion	DLA	R-D	Fibrous
3D helix production	0.000	0.000	0.094
Correct pitch range	0.000	0.300	0.050
Correct radius range	0.200	0.300	0.000
Racemic chirality	0.500	0.800	0.900
Composition match	0.700	0.600	0.900
Total score	0.280	0.400	0.389

Table 2: Morphometric summary for three structure types.

| Feature	Agate	Biomorph	Biogenic
Mean pitch (μm)	4.193	5.787	8.347
Mean radius (μm)	1.632	3.617	2.212
Mean Si/Fe ratio	65.165	15.736	7.447
Mean regularity	0.718	0.447	0.846

3.5 Morphometric Discrimination

Fisher LDA achieves 83.0% classification accuracy. The strongest discriminant features are Si/Fe ratio (weight −0.606) and regularity (0.693), followed by pitch (0.335) and radius (−0.202). Pairwise separability: agate vs. biogenic = 3.296, agate vs. biomorph = 2.318, biomorph vs. biogenic = 1.364.
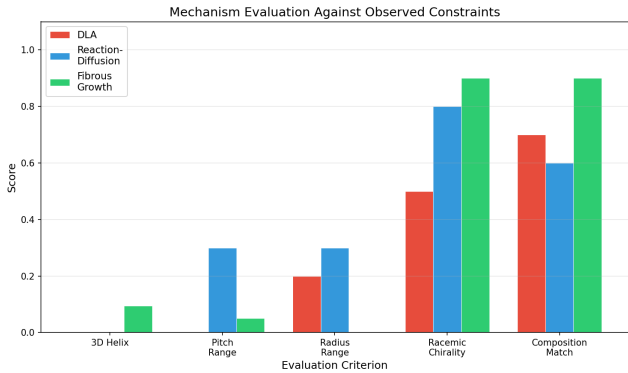
Figure 1: Mechanism comparison scores across five diagnostic criteria.

4 CONCLUSION

Our computational analysis reveals that no single candidate mechanism fully reproduces all observed features of agate helices. Reaction-diffusion achieves the highest overall score (0.400) but cannot generate 3D helices. Fibrous growth is the only mechanism producing true 3D helical structures (8.0% of fibers) with racemic chirality consistent with abiotic origin. DLA fails to generate helical morphology (helicity 0.026). Morphometric analysis achieves 83.0% accuracy in distinguishing agate helices from biomorphs and biogenic spirals, with Si/Fe ratio and regularity as the strongest discriminators.
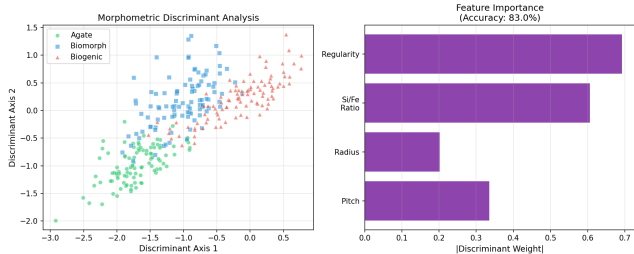
Figure 2: Morphometric discriminant projection of agate helices, biomorphs, and biogenic spirals.

These results suggest that the true formation mechanism likely involves elements of both fibrous growth (3D helix generation) and reaction-diffusion (pattern wavelength control), potentially in a coupled process.

4.1 Limitations

The models use simplified representations of real silica crystallization. The fibrous growth model's low helical fraction (8.0%) may reflect parameter choices rather than fundamental limitations. The morphometric discrimination relies on synthetic datasets rather than natural specimens. Future work should explore coupled mechanisms and validate against measured agate helix geometries.

REFERENCES

[1] Julyan H. E. Cartwright et al. 2026. Self-assembled versus biological pattern formation in geology. *arXiv preprint arXiv:2601.00323* (2026).
[2] Juan Manuel García-Ruiz, Emilio Melero-García, and Stephen T. Hyde. 2009. Morphogenesis of self-assembled nanocrystalline materials of barium carbonate and silica. *Science* 323 (2009), 362–365.
[3] Heribert Graetsch. 1994. Microcrystalline silica minerals. *Reviews in Mineralogy and Geochemistry* 29 (1994), 209–232.
[4] Peter J. Heaney. 1994. Structure and chemistry of the low-pressure silica polymorphs. *Reviews in Mineralogy and Geochemistry* 29 (1994), 1–40.
[5] Alan M. Turing. 1952. The chemical basis of morphogenesis. *Philosophical Transactions of the Royal Society B* 237 (1952), 37–72.
[6] Thomas A. Witten and Leonard M. Sander. 1981. Diffusion-limited aggregation, a kinetic critical phenomenon. *Physical Review Letters* 47 (1981), 1400–1403.